Integration of HVSR measures and stratigraphic constraints for seismic microzonation studies: the case of Oliveri (North-Est Sicily)

Di Stefano P.[1], Luzio D.[1], Renda P.[1], Martorana R.[1]*, Capizzi P.[1], D'Alessandro A.[1], Messina N.[1], Napoli G.[1], Todaro S.[1], Zarcone G.[1]

[1] *Dipartimento di Scienze della Terra e del Mare - DiSTeM, University of Palermo, Italy*

* raffaele.martorana@unipa.it

Abstract

Because of its high seismic hazard the urban area of Oliveri has been subject of first level seismic microzonation. The town develops on a large coastal plain made of mixed fluvial/marine sediments, overlapping a complexly deformed substrate. In order to identify points on the area probably suffering relevant site effects and define a preliminary V_s subsurface model for the first level of microzonation, we performed 23 HVSR measurements. A clustering technique of continuous signals has been used to optimize the calculation of the HVSR curves. 42 reliable peaks of the H/V spectra in the frequency range 0.1-20 Hz have been identified. A second clustering technique has been applied to the set of 42 vectors, containing Cartesian coordinates, central frequency and amplitude of each peak to identify subsets which can be attributed to continuous spatial phenomena. The algorithm has identified three main clusters that cover significant parts of the territory of Oliveri. The HVSR data inversion has been constrained by stratigraphic data of a borehole. To map the trend of the roof of the seismic bedrock, from the complete set of model parameters only the depth of the seismic interface that generates peaks fitting those belonging to two clusters characterized by lower frequency has been extracted.

The reconstructed trend of the top of the seismic bedrock highlights its deepening below the mouth of the Elicona Torrent, thus suggesting the possible presence of a buried paleo-valley.

1. Introduction

The seismic microzonation of a territory aims to recognize the small scale geological and geomorphological conditions that may significantly affect the characteristics of the seismic motion, generating high stress on structures that could produce permanent and critical effects (site effects) (Ben-Menahem and Singh, 1981; Yuncha and Luzon, 2000). The first phase of the seismic micro-zoning is the detailed partition of the territory in homogeneous areas with respect to the expected ground shaking during an earthquake.

The dynamic characteristics of a seismic phase of body or surface waves, generated by an earthquake and incident on a portion of the ground surface, often show sharp variations, frequency dependent, sometimes having extremely local character.

Significant increases in amplitude of the phases for which occur peak values of the kinematic parameters of ground shaking, are called site effects. In general all this phenomena are controlled by anomalies in the mechanical properties of the shallowest layers of subsoil, when it consists of soft sediments, or by the shape of surfaces of discontinuity close to or coincident with the topographic surface.

If we knew a very detailed mechanical model of the cover layer, consisting of soft sediment, we could predict the site effects or even determine univocally its transfer function by means of numerical calculation.

The difficulty and costliness of the reconstruction of a suitable model of subsurface using geophysical techniques and the necessity of not neglecting nonlinear effects (Dimitriu et al., 2000) have led many researchers to develop and adopt more direct techniques that allow to determine approximated empirical transfer functions.

Nakamura (1989) proposed that in correspondence to the resonance frequencies of a sequence of layers, the Horizontal to Vertical Spectral Ratio (HVSR) of the seismic noise presents peaks well correlated with the amplification factor of S waves, generated by earthquakes, between the bottom and the roof of the stratification.

Not necessarily, however, an HVSR peak must be attributed to resonance frequencies of a buried structure, it might also depend on characteristics of the sources of noise and in such case it will be not correlated with amplification effects on incident waves trains.

In fact, one of the most controversial aspects in the application of the HVSR technique concerns the criteria for the selection, in the microtremor signals, of appropriate time windows for the calculation of the HVSR curves. However, an appropriate techniques based on an Agglomerative Hierarchical Clustering (AHC) algorithm may help to discriminate, between peaks caused by source effects and those due to site effects (D'Alessandro et al., 2013). The separation of the two effects can allow to determine for each cluster an average HVSR curve better related to the local site effects and to identify all the significant peaks of the H/V spectra in the chosen frequency range.

Another problematic aspect must be addressed when the HVSR method is applied for the seismic microzonation of an area, that is, for its subdivision into relatively uniform areas with respect to their response to a seismic input. Each HVSR curve may contain more significant peaks attributable to different causes namely different characteristics of the subsurface.

The cluster analysis can be used to group HVSR peaks probably due to the same site effect, for example a seismic reflector or a topographic effect.

In each interior point to an area identified by each cluster, it will be reasonable to assume a same site effect and characterize it in frequency and amplitude with a technique of 2D interpolation of parameters determined at the measurement points.

Although it is not possible to exclude that the frequencies belonging to the same cluster are due to different structures or vice versa, the depth values obtained by inverting the average HVSR curves, if related to peaks of the same cluster, can be interpolated to reconstruct the same seismic reflector.

2. The study region

2.1. Geological setting

The area of Oliveri is part of the Peloritani Mountains, a segment of the Siculo-Maghrebian chain that is mainly constituted by a pile of tectonic units consisting of Hercynian metamorphic rocks and their Meso-Cenozoic sedimentary covers (Giunta et al., 1998, cum biblio).

In the Peloritani Mountains different deformation steps are related to the Alpine orogeny, superimposed to Hercynian ductile deformations. The Oligo-Miocene contraction has been characterized by several phases in which there has been the formation of folds associated with thrust systems that fragmented and stacked the crystalline rocks and their sedimentary covers in different tectonic units.

Reverse fault systems (breaching) affected the area since the Upper Miocene resulting in moderate shortening (Giunta & Nigro, 1998). At the end of the Miocene the Tyrrhenian rifting produced a series of extensional low angle faults that resulted in a thinning of the chain. During Plio-Pleistocene times the area occupied by the Peloritani Mountains was affected by a strike-slip tectonic phase that generated two different systems: the first one synthetic with right cinematic and oriented NO-SE and E-O; the second one antithetical, mainly sinistral and oriented N-S and NE-SW (Ghisetti & Vezzani, 1977; Nigro & Renda, 2002).

Around the Oliveri plain there is evidence of active tectonics characterizing a right-lateral shear zone named Aeolian-Tindari-Letojanni fault (Ghisetti, 1979). This fault is generated by two different geodynamic domains: compressive to west, related to a roughly N-S trusting produced by continental collision, and extensional to east, controlled by NW-SE expansion of the Calabro-

Peloritan Arc (De Guidi et al., 2013). The analysis of seismic and geodetic data, acquired in the last 15 years, and structural and morphological surveys show evidence of tectonic activity in this area to as recent as the middle-upper Pleistocene (Catalano & Di Stefano, 1997; Ghisetti, 1979; De Guidi et al., 2013). Recent studies, not far from the Oliveri plain, have characterized some geothermal springs and gas vents and discussed their possible role in the generation of earthquakes (Giammanco et al., 2008) and on the basis of paleontological data, have estimated a very high rate of uplift, up to 5,5 mm/year (Di Stefano et al., 2012).

The lithostratigraphic framework of the substrate of the urban area (Fig. 1) is made up by the metamorphic basement of the Aspromonte Unit that is covered unconformably by the arenaceus member of the Capo D'Orlando Flysch. Upwards the flyschoid sediments are tectonically overlaid by the Argille Scagliose Antisicilide. The previous deposits are capped by sands and calcarenites of Plio-Pleistocene age. The most recent sediments consists of alluvial and beach deposits.

2.2. Regional Seismicity

The Oliveri territory is located in the area 932 of the ZS9 seismogenic zonation of Italy (Meletti and Valensise 2004). It includes seismogenic structures largely known through geophysical exploration. The faults in this area partly allow the retreat of the Calabrian Arc and some are synthetic faults that segment the Gulf of Patti. The area 932 is one of the areas with the highest seismic potential of the whole Sicily. In it the earthquake of 1908 occurred, for which different source mechanisms have been proposed, some of which are, probably, associated with the activation of complex fault systems or blind faults (Ghisetti 1992; Valensise and Pantosti 1992; Monaco and Tortorici 1995).

The high rate of seismicity in the Gulf of Patti and in the area between Alicudi and Vulcano is associated to the two right-slip fault systems, Patti-Volcano-Salina and Sisyphus, respectively oriented NW-SE and WNW-ESE. The most energetic instrumental earthquakes have occurred in this area April 15, 1978 and May 28, 1980 with a local magnitude of 5.5 and 5.7 respectively.

The earthquake of 1978 (MW = 6.6), related to movements along these faults (Neri et al., 1996), caused considerable damage in many countries of the Messina province and was felt up to the Cosenza province in the north, to Dubrovnik in the south, to Trapani to the west and to the Ionian coast of Calabria to the east. The estimated maximum macroseismic intensity has been VIII-IX MCS. Its mean macroseismic intensity in the Oliveri area was VII MCS, where it caused serious damage in some buildings and significant soil fractures (Barbano et al., 1979).

The earthquakes of Novara di Sicilia, with lower magnitude and shallower hypocenters, seem to be linked to structures other than the fault system Patti-Volcano-Salina. The earthquakes of Naso might instead be associated with NE-SW normal faults responsible for the lifting of the chain. Among the structures present in the southern Tyrrhenian sea, those oriented around EO, would be responsible for the events of the western sector of the Aeolian Islands, and may have generated earthquakes like the one in 1823.

Neri et al. (2003) have determined the focal mechanisms of earthquakes with depths less than 50 km, occurred in Calabria and Sicily between 1978 and 2001. These indicate a high heterogeneity of the deformation field in the area 932. Here the deformation style ranges from extensional with southwest exposure to compressional with northeast exposure, proceeding from SE to NW.

The first earthquake with a destructive effect in the Oliveri area, reported in the catalogs of historical Italian seismicity, occurred in March 10, 1786. This seismic event was characterized by $M_W = 6.1 \pm 0.4$, epicenter at Oliveri and MCS intensity equal to IX in the urban area. This earthquake severely damaged all the cities of the Gulf of Patti in northern Sicily and almost destroyed the town of Oliveri (Guidoboni et al., 2007).

The seismic activity recorded in the last 20 years in the area surrounding the urban center of Oliveri, represented in Figure 2, is characterized by about 3500 events with local magnitude greater than 2. Of these about 89% have hypocenters tightly concentrated around an average depth of about 10 km. The remaining 11% consists of events whose hypocenters are thickened around a plane that

dips toward the northwest at an angle of about 60° and are distributed rather uniformly with respect to depths up to 400 km. The sources of these events are located inside the Ionian lithospheric slab that dips under the Calabrian Arc (Giunta et al., 2004).

An analysis of completeness of these data sets has indicated a local magnitude threshold equal to about 2.6 (Schorlemmer et al., 2010; D'Alessandro et al., 2011).

The shallow seismic activity has a marked tendency to occur through sequences of aftershocks sometimes preceded by foreshocks. This tendency was assessed in a quantitative way by comparing the estimates of the correlation dimension in the domains of the epicenter coordinates and time, both for the component of the seismicity constituted by events not followed by aftershocks and the main shock of the sequences that for the total set of events (Adelfio et al., 2006). The estimates of the space and time correlation dimension relating to independent events are close to those expected for uniform distributions, as opposed to those for the total set that are much smaller.

The geometric characteristics of the clusters related to the shallower seismicity identify orientations that are consistent with those of the main tectonic structures of the area.

The seismicity of the last 20 years has also been analyzed in the magnitude domain. For the events of the area of Figure 2 the value of b of the law of Gutenberg-Richter and the 95% confidence interval have been estimated, using the estimator of Tinti and Mulargia (1987) not distorted by the data grouping. In particular, for deeper events, associated with the Ionian slab, the value of b is equal to 0.6±0.2 while for superficial events the value 1.15±0.13 has been estimated, which is comparable with the value obtained for the independent component of the seismicity of the whole south - Tyrrhenian area (see Adelfio et al., 2006).

3. HVSR measurements

3.1. Background and points under discussion

To try to identify areas of the town of Oliveri probably interested in site effects and to define a preliminary subsurface model 23 HVSR measurements have been performed, quite uniformly distributed with a mean spacing of about 250 m.

For the measurements the 3 component seismic digital station TROMINO® (Micromed) has been used, equipped with three velocity transducers.

For each measurement point the recording length was 46 minutes and the sampling frequency 256 Hz. Each recording was subdivided in windows of 50s long. This choice allowed us to have the minimum number of windows selected for the analysis according to Sesame (2004). Following the SESAME criteria, the signal relative to each time window was de-trended, baseline corrected, tapered and band pass filtered between 0.1 and 25 Hz. Than we performed the FFT of each signal components and determined the HVSR curve following Konno and Ohmachi (1998). The analysis were limited to the range 0.1-20 Hz, which is the frequency range of interest for seismic microzonation and earthquake engineering. The data in the frequency domain have been filtered with a triangular window to obtain a smoothing of 10%. The attribution of peaks to resonance phenomena of buried structures has been validated, in agreement with SESAME criteria, by analyzing the standard deviation of the spectral amplitudes and the independence from the azimuth of the mean spectral ratio (Fig. 3). Assuming an approximately one-dimensional ground around each measurement point, a peak of the HVSR curve should be attributed to characteristics of the subsoil only if it is azimuthally stable.

In order to obtain reliable HVSR curves, several acquisition and processing criteria must be adopted. The most important criteria concern the acquisition modes and those of extraction, from a continuous record, of an optimal set of analysis time windows, for the evaluation of a HVSR function, dominated by the effects of buried geological structures (SESAME Project, 2004). This last is probably the most controversial aspect in the HVSR technique implementation. Several authors believe that spikes and transients in microtremors bring information highly dependent from the sources and therefore cannot be used to estimate resonance frequencies of sites (Horike et al.,

2001; SESAME Project, 2004). Therefore, they exclude the non-stationary portion of the recorded noise, thus considering only the low-amplitude part of signal, for the computation of the average HVSR function. Other authors, instead, (Mucciarelli and Gallipoli, 2004) suggest that the non-stationary large-amplitude noise windows should not be removed, because these, generally, carry subsoil information that improves the correlation between the noise and earthquakes HVSR curves.

The windows selection can be made in both time and frequency domain. In time domain, the eligible windows are identified by inspecting the three components of the signal. In frequency domain the windows are selected, determining the spectral ratios in consecutive time windows, and subsequently selecting the HVSR curves that, at sight, seem to be more similar to each other. Clearly, the second approach bypasses the problem of the choice of time windows containing only the low-amplitude fraction of noise or also high-energy transients. However, the selection of the windows is still done in an arbitrary way. The use of the visual inspection technique practically make the processing long and farraginous, the result is strongly dependent by the skill of the operator, while its reliability is difficult to assess quantitatively.

In a first level seismic microzonation, after the identification for each investigated point of the peaks of the HVSR curves attributable to resonance effects of the site, it is necessary to delineate areas of similar behaviour in seismic perspective. The identification of these areas involves the simultaneous assessment of several parameters such as the frequency and amplitude of the resonance frequencies, and the positions and the mutual distances between the measuring points. The task becomes particularly difficult when it is possible to identify on the HVSR curves different peaks associable with different resonance frequencies of the investigated site.

To overcome the aforementioned problems, we have implemented two automatic procedures based on cluster analysis.

3.2. Implementation by cluster analysis

Cluster analysis is the task of grouping a set of objects in such a way that objects in the same group (called cluster) are, in some sense, more similar to each other (internal cohesion), than to those in other groups (external isolation). It is a main task of exploratory data mining, and a common technique for statistical data analysis.

Clustering is, typically, an unsupervised process and the results of the application of different algorithms to the same data set, may be very different from each other, thus the assessment of the clustering algorithms is fundamental. Several clustering validation approaches have been developed (Gan et al., 2007; Everit, et al., 2011), mainly based on the concepts of homogeneity and separation. We used as measure of cluster quality the variance decomposition method using the *within-class* and the *between-classes* variances as measure of homogeneity and separation, respectively (Gan et al., 2007; Everit, et al., 2011). A good clustering should identify a small number of clusters characterized by a within-class variance less than of the between-classes one. Both the procedure proposed are based on the Hierarchical Clustering (HC) Algorithms (Gan et al., 2007; Everit, et al., 2011). The HC algorithms are explorative methods for which it is not necessary to fix a priori the number of clusters. HC methods work with a measure of proximity between objects to be clustered. The proximity measure has to be chosen, so that it is suited to the nature of the data.

Hierarchical clustering algorithms can be agglomerative or divisive. In the Agglomerative Hierarchical Clustering (AHC), or bottom-up approach, each object begins the process as the only member of its own cluster and the process is concluded with the inclusion of all the objects in a single cluster; in the Divisive Hierarchical Clustering (DHC), or top-down approach, instead, all observations are initially placed in a single cluster, which is subdivided iteratively until to obtain N clusters. Application of both AHC and DHC verifies that the two algorithms leads to very similar solutions, but the first kind of processing is less time-consuming.

To address the two problems above described both the implemented procedures are based on the AHC algorithm and used the Average Linkage (AL) criterion, in which the dissimilarity between the objects A and B is the average of the dissimilarities between the objects of A and the

objects of B (Gan et al., 2007; Everit, et al., 2011). This has been chosen because, besides providing a fair representation of the data space properties, in our tests the best results in terms of variance decomposition and stability of the solutions were obtained.

Several measure of proximity between two elements of the set were proposed in literature to measure the similarity/dissimilarity of different kinds of objects (Gan et al., 2007; Everit, et al., 2011). Clearly, the choice of the type of proximity measure must respect specific criteria and should be optimized depending on the type of data and aim of clustering (Gan et al., 2007; Everit, et al., 2011).

For the identification of the optimal set of analysis windows for the determination of the average HVSR curve, we have adopted as a measure of proximity the Standard Correlation (SC_{xy}) defined as:

$$SC_{xy} = \frac{\sum_{i=1}^{n} x_i \cdot y_i}{\sqrt[2]{\sum_{i=1}^{n} x_i^2 \cdot \sum_{i=1}^{n} y_i^2}} \quad (1)$$

were x_i and y_i indicate the values of the spectral ratios relative to the i-th frequency and the generic pair of analysis time windows x and y. It takes into account both the position and amplitude of the peaks present on the HVSR curves.

To define clusters of HVSR peaks, representative of measurement points, with the aim of defining homogeneous areas in seismic perspective, it is important that the process of clustering takes into account all the parameters involved; these are clearly the period and the amplitude of each peak. In addition to these parameters, we could consider also the values of the same parameters in the neighbouring points. For this reasons, in the implemented clustering procedure, we have defined the following proximity measure:

$$S_{ij} = 1 - \left(\alpha T_{ij} + \beta A_{ij} + \gamma D_{ij}\right); \quad \text{with } \alpha + \beta + \gamma = 1 \quad (2)$$

where T_{ij}, A_{ij} and D_{ij} are normalized Euclidean distance in the parameters space (period, amplitude and measurement position, respectively) and α, β and γ are weights to be assigned to the respective distances. These parameters are reported in Table 1. The results of the analysis carried out are summarized in dendrograms and the variance decomposition was adopted as optimal criterion for the choice of the proximity cut levels.

4. Frequency maps

The HVSR data (Fig. 4) have revealed the likely presence of amplification of ground motion in the frequency range 0.7÷1.6 Hz, over a large part of the urban area. The thickness of the soft coverage in few places where it is known and its lithological composition allow us to hypothesize that the cause of amplification is the resonance of the same coverage.

The clustering procedure used to group peaks of HVSR average curves related to different sites, has allowed to identify areas characterized by site effects probably caused by the same buried structure. Considering the parameters of such peaks as sampling of spatial trends that are continuous on the area containing the measuring points, it is possible to estimate the expected peak amplitude and frequency at each point of the area by two-dimensional interpolation techniques.

In the cluster algorithm the elements of the similarity matrix are weighted averages of Euclidean relative distances between the quantitative parameters of a pair of peaks, and each difference between pairs of parameters is normalized by the maximum difference in the sample. To avoid the inclusion in the same cluster of more peaks relative to the same measurement point, the normalized relative distance of coincident points was placed equal to 1.

The choice of the weights to be assigned to the equation (2) should be made on the basis of the statistical parameters that allow to quantify the goodness of the clustering procedure, such as

homogeneity and separation of the clusters, but also on the basis of importance and reliability of each parameter.

The resonance period of a site is a very important parameter and surely the most robust one that can be estimated from the HVSR curve. The resonance period is linked to the local geology in term of S-wave velocity and thickness of the resonant layer. On the other hand, the associated amplitude value is not a robust parameter. In fact, only if the microtremors wave-field consist of body waves the shape of the HVSR curves is mainly controlled by the S-wave transfer of the shallowest sedimentary layers and the peaks amplitude may be straightforward related to subsoil amplification factors. The topographical distance is instead a parameter of high importance, both for the identification of homogeneous areas in seismic perspective, but also as an indirect measure of the reliability of peaks of the HVSR curves associated to resonance effects.

In order to identify the optimal weights values in our clustering procedure we have tried to cluster our data using all the possible combinations of weights ranging between 0.2 and 0.5, with step of 0.1. The values of weights able to provide the best result in term of variance decomposition (minimum within-class and maximum between-classes variance) were the following: α=0.4, β=0.2 and γ=0.4.

The procedure of clustering made it possible to split the total set of peaks in four clusters referred to as: B (Blue), R (Red), G (Green), V (Violet), respectively, consisting of 21, 12, 7, and 2 peaks. The cluster made up of only two peaks has been neglected in the overall description of the area due to poor reliability of both peaks, highlighted by the parameters listed in Tab. 1. Fig 5 shows the dendrogram of the clustering process. From this it is clear that, adopting a cut threshold slightly lower than the optimal one adopted by the calculation code, the three remaining clusters would be gathered in a single cluster. Different criteria can be used to find the optimal threshold. In this paper, the optimal threshold was identified seeking in the dendrogram the large gap between two successive levels of the hierarchy.

Fig. 6 shows the characteristics of the clusters in the diagram H/V vs. period and the spatial distribution of B, R and G clusters.

As the two clusters B and G are very near in the scatter plot and their areas have an empty intersection, it was considered reasonable to assume that they represent the effects, continuously variable on the union of their areas, of a single source phenomenon. In particular it is assumed that B and G are related to the resonance effect of a covering layer delimited at its base by the same discontinuity surface with variable depth. Conversely it is assumed that the cluster R, whose extent represent a significant part of that of B$\cup$G and is characterized by higher frequencies respect to the corresponding ones of the peaks of B$\cup$G, show the resonance effects of the sedimentary cover down to a shallower interface.

Therefore, two different maps can be reconstructed, each of them grouping and separately representing the continuous trend of the frequency for the clusters A$\equiv$B$\cup$G and R. The amplification estimated at the measurement points is reported numerically in the maps, being not reliably mappable with smoothed trends over large areas.

For the processing of the maps, the kriging algorithm has been applied to interpolate the experimental peak frequencies at the nodes of a regular lattice with spacing equal to 10 m. The frequency maps are plotted using a contour equidistance equal to 0.05 (Fig. 7).

An area south of the town, interesting for the spatial planning, seems to be characterized by higher amplification at frequencies greater than 1.2 Hz (Fig. 7, right).

5. Bedrock mapping by inversion of HVSR measurements

The determination of the parameters that characterize the subsoil from the H/V curves provides unreliable results if you don't use an initial model already representative of the real geological stratification, well constrained by drilling data, geological observations or results of other geophysical surveys.

It should be, also, pointed out that, due to lateral variations of geologic parameters as: porosity, water content, fracturing degree, etc. the mechanical parameters of each layer will not be uniformly distributed with obvious negative consequences on the accuracy of the estimate of the depth of geological interfaces and in particular the roof of the seismic bedrock.

Taking into account the available geological information, the H/V curves have been inverted to estimate the depth of the seismic bedrock, also reported in Table 1.

The inversion has been carried out using the Dinver inversion code, developed in the frame of the project Geopsy (Wathelet et al., 2004; Wathelet 2008). In this technique the computation of the dispersion curve for a stack of horizontal and homogeneous layers is determined (Haskell, 1953). Only the Rayleigh phase velocities are considered as the experimental dispersion curve is generally obtained from processing the vertical components of noise. A limit of this method lies in the uncertain composition of seismic noise and in the impossibility to include among the unknown parameters those relating to the model of the microseismic field (Peterson, 1993). For the inversion the neighbourhood algorithm (Sambridge 1999) was used. This is a stochastic direct-search method for finding models of acceptable data fit inside a multidimensional parameter space.

Unfortunately, it has been possible to constrain the model using only the data of a single borehole, located at the eastern boundary of the municipality (fig. 8), to impose constraints on the thicknesses of the layers in the inversion of the HVSR curve related to the nearest recording point. We considered reliable inverse models with misfits about equal or less than 1. Misfits were calculated as a sum of squared differences between observed data and calculated ones, normalized by the variance.

To define the starting model for the inversion, the values of shear-wave velocity of the cover available for the studied area were used. In particular, we considered about 200 to 250 m/s for alluvium and about 350 to 400 m/s in correspondence of silty sands.

The depth of transition of the shear wave velocity from less to greater than 800 m/s is considered the depth of the seismic bedrock. When evaluating the reliability of the estimate of this depth, we must consider that the trends represented are heavily influenced by the interpolation process between the HVSR measuring points. The depth values obtained from every measuring points are in fact only possible estimates, assuming minimal lateral variations. To avoid interpolation between depths of interfaces due to different geological structures, it was decided to group and correlate frequencies related to the same cluster. However it is not possible to exclude that frequencies belonging to the same cluster are due to different structures or vice versa.

In almost all the HVSR measurements carried out on the alluvial material a maximum peak is mostly evident in the range 0.7 - 1.4 Hz (Fig. 4). This, by the inversions results, seems to be related to a variation of the shear-wave velocities that, under a depth of 40-60 meters reach values attributable to a seismic bedrock (about 800 m/s).

Analyzing the 1D inverse models (fig. 9) derived by inverting HVSR measurements, estimates of the depth of the seismic bedrock have been obtained. These, together with other reliable data like drilling and other geophysical surveys, were used to construct the map of the thickness of the sedimentary cover (Fig. 10, left) and the map of the altitude of the top of seismic bedrock above sea level (Fig. 10, right). The estimates of the depth of the bedrock were interpolated by imposing a constraint of a depth equal to zero in areas where geological strata with elastic characteristics of seismic bedrock outcrop. The kriging interpolation algorithm was used, obtaining a lattice with equidistance between nodes equal to 10 m.

The map of the bedrock depth contours was obtained by extracting from the Digital Elevation Model of the area a grid of points equidistant 50 m. From these the corresponding lattice of the depth of the bedrock were subtracted. This choice was made in order to obtain a trend of the

isobaths that was not excessively tied to topographic detail but which, however, did not present unrealistic areas with higher elevations of the topographic surface. It should however emphasize that the real detail of the maps can't be higher than the sampling density of the HVSR measurements, which generally is not less than 300 m.

6. Geological interpretation

Considering the geological configuration of the subsoil and the values of shear-wave velocity a preliminary identification was made of the geological structures that can cause seismic resonance.

It was not possible to define the lithological distribution in particular under the town, for the lack of well data. Only the data from two wells have been used; the first is located close to Torrente Elicona (Fig. 8), the second is located close to the Castello hill. The analysis of the core of the first one shows the presence of anthropic deposits in the first 1.6 m, followed by 3.4 m of well graded sand with gravel elements of metamorphic origin, 5.5 m of silty sand, with rare rounded gravel elements, and 5.4 m of poorly graded sand. The altered substrate, according to its mechanical characterization by HVSR data, seems to be made by incoherent sand and grey silt. The analysis of core samples permitted to recognize bivalve fauna. The groundwater level is placed at a depth of 7.5 m.

The core relative to the second well shows evidence of a tectonic dislocation that put in contact the “Argille Scagliose” unit with the metamorphic basement. In the northern side of Torrente Castello, the flyschoid cover has a thickness of about 20 m while, in the southern part, the thicknesses of clay and calcarenite covers exceed 45 m (Fig.10). The nature of the covers is related to the sedimentary contribution of the rivers and sea level fluctuations.

On the basis of the 3D trend of seismic bedrock and of geological information from field surveys and from published geological maps, three geological sections were drawn (fig. 11).

In the section A, oriented from west to east, it is possible to observe, in the westernmost part, the stratigraphic overlay of the Flysch of Capo D'Orlando on the metamorphic substrate, which is lowered eastward by normal faults. The alluvial deposits of coastal plain are onlapping on the substrate whose lithology is not known in most of the area (sections B and C in fig. 11) due to the lack of information deriving from deep boreholes. Therefore the only information is related to geophysical analysis. Finally, along the Oliveri plain some catalogs (e.g. ITHACA) and structural studies (Ghisetti & Vezzani, 1977) testify the presence of an active fault that in geological sections is approximately shown.

The reconstructed model suggest the presence of two buried river bed separated by a relief. The sediment thickness in these two areas is about 45 m. In the seismic bedrock map (Fig. 10, right) is possible to observe as the rivers bed suffer a migration toward the present day position. According to the bedrock map the relief that separates the two depressions has a depth of 40 m while the floor of basins show a depth of 60-70 m. In the southern part of the town there is another basin in which the bedrock has a deepness of 40 m. This could be related to another minor river joined with Torrente Elicona. Based on hydrogeological information the presence of groundwater level in the floodplain is attested at a depth less than 15 m. This condition renders the floodplain exposed to liquefaction risk.

7. Conclusions

The application of a first clustering procedure to the set of HVSR data allowed to separate in different clusters the noise windows with spectral effects due to subsurface structures and those dominated by accidental interference effects between waves trains of a different nature.

The average spectral ratio of the cluster dominated by structural effects, often has been characterized by smaller variance of the frequencies and amplitudes of the significant peaks, compared to those of the peaks determined with standard methods.

A second clustering procedure applied to estimated frequencies and amplitudes of the peaks, allowed to identify areas where it could be considered realistic to interpolate the peak parameters linked to the same buried structures.

Assuming that the three main identified clusters contain peaks produced by resonance effects of layers with varying thickness, the possible trend of the roof of the seismic bedrock was reconstructed by inversion of the HVSR curves constrained with geological and lithological information and considering a minimum lateral variability of the physical and geometrical parameters. The reliability of the 3D model obtained is limited by the lack of geophysical and drilling data, which would have allowed us to better constrain the values of the unknown parameters of the model. However, the general characteristics of the reconstructed subsoil are fully compatible with the geological model of the area. The necessary surveys to increase the resolution and reliability of the model will be carried out in more detailed studies provided by the microzoning of second and third level.

References

Adelfio, G., Chiodi, M., De Luca, L., Luzio, D., and Vitale, M.: *Southern-Tyrrhenian seismicity in space-time-magnitude domain,* Annals of Geophysics, 49 (6), pp. 1245-1257, 2006

Barbano, M.S., Bottari, A., Carveni, P., Cosentino, M., Federico, B., Fonte, G., Lo Giudice, E., Lombardo, G., and Patanè, G.: *Macroseismc study of the gulf of Patti earthquake in the geostructural frame of the North-Eastern Sicily*, Bollettino della Società Geologica Italiana, 98, 155-174, 1979.

Ben-Menahem, A. and Singh, S.J.: Seismic Waves and Sources, Springer-Verlag, New York, 1981.

Catalano, S. and Di Stefano, A.: *Sollevamenti e tettogenesi pleistocenica lungo il margine tirrenico dei Monti Peloritani: integrazione dei dati geomorfologici, strutturali e biostratigrafici*, Il Quaternario (Italian Journal of Quaternary Sciences) 10 (2), 337–342, 1997.

D'Alessandro, A., Capizzi, P., Luzio, D., Martorana, R., and Messina, N.: *Improvement of HVSR technique by cluster analysis*. Geoitalia 2013, IX FIST, Pisa, 16-18 Settembre 2013, 2013.

D'Alessandro, A., Luzio, D., D'Anna, G., and Mangano, G.: *Seismic Network Evaluation through Simulation: An Application to the Italian National Seismic Network*, Bulletin of the Seismological Society of America, DOI: 10.1785/0120100066, 101 (3), 1213-1232, 2011.

De Guidi, G., Lanzafame, G., Palano, M., Puglisi, G., Scaltrito, A., and Scarfì, L.: *Multidisciplinary study of the Tindari Fault (Sicily, Italy) separating ongoing contractional and extensional compartments along the active Africa-Eurasia convergent boundary*, Tectonophysics, 588, 1-17, 2013.

Di Stefano, E., Agate, M., Incarbona, A., Russo, F., Sprovieri, R., and Bonomo, S.: *Late Quaternary high uplift rates in northeastern Sicily: evidence from calcareous nannofossils and benthic and planktonic foraminifera*, Facies, 58, issue 1, 1-15, 2012.

Dimitriu, P., Theodulidis, N., and Bard, P.Y.: *Evidence of non linear site in HVSR from SMART1 (Taiwan) data*, Soil Dynamicsand Earthquake Engineering, 20, 155-165, 2000.

Ghisetti, F.: *Relazioni tra strutture e fasi trascorrenti e distensive lungo i sistemi Messina-Fiumefreddo, Tindari-Letojanni e Alia-Malvagna (Sicilia nord-orientale): uno studio microtettonico*. Geol. Rom., 18, 23-58, 1979.

Ghisetti, F.: *Fault parameters in the Messina Strait (southern Italy) and relations with the seismogenic source*, Tectonophysics, 210 (1-2), 117-133, 1992.

Ghisetti, F. and Vezzani, L.: *Evidenze di linee di dislocazione sul versante meridionale dei Monti Nebrodi e Madonie e loro significato neotettonico*, Boll. Geodesia e Sc. affini, 36 (4): 411-437, 1977.

Giammanco, S., Palano, M., Scaltrito, A., Scarfì, L., and Sortino, F.: *Possible role of fluid overpressure in the generation of earthquake swarms in active tectonic areas: the case of the Peloritani Mts. (Sicily, Italy)*, Journal of Volcanology and Geothermal Research 178, 795–806, 2008.

Giunta, G., Messina, A., Bonardi, G., Nigro, F., Somma, R., Cutrupia, D., Giorgianni, A., and Sparacino, V.: *Geologia dei Monti Peloritani (Sicilia NE)*, Guida all'escursione, 77° Riunione estiva, Palermo, 1998.

Giunta, G. and Nigro, F.: *Some tectono-sedimentary constraints to Oligo-Miocene evolution of the Peloritani Thrust Belt*, Tectonophysics, 315: 287-299, 1998.

Giunta, G., Luzio, D., Tondi, E., De Luca, L., Giorgianni, A., D'Anna, G., Renda, P., Cello, G., Nigro, F., and Vitale, M.: *The Palermo (Sicily) seismic cluster of September 2002, in the seismotectonic framework of the Tyrrhenian Sea-Sicily border area,*. Annals of Geophysics, 47 (6), 1755-1770, 2004.

Guidoboni, E., Ferrari, G., Mariotti, D., Comastri, A., Tarabusi, G., and Valensise, G.: *Catalogue of Strong Earthquakes in Italy (CFTI), 461 B.C. - 1997 and Mediterranean Area 760 B.C. - 1500*, http://storing.ingv.it/cfti4med/, 2007.

Horike, M., Zhao, B., and Kawase, H.: *Comparison of site response characteristics inferred from microtremors and earthquake shear waves*, Bulletin of the Seismological Society of America, 91 (6), 1526-1536, 2001.

Konno, K. and Ohmachi, T.: *Ground-Motion Characteristics Estimated from Spectral Ratio between Horizontal and Vertical Components of Microtremor*, Bull. Seism. Soc. Am., 88:1, 228-241, 1998.

Meletti, C. and Valensise, G.: *Zonazione sismo genetica ZS9 – App.2 al Rapporto Conclusivo*, http://zonesismiche.mi.ingv.it/documenti/App2.pdf, 2004.

Monaco, C. and Tortorici, L.: *Tectonic role of ophiolite-bearing terranes in the development of the southern Apennines orogenic belt*, Terra Nova, 7 (2), 153-160, 1995.

Mucciarelli, M. and Gallipoli, M.R.: *The HVSR technique from microtremor to strong motion: empirical and statistical considerations, 13th World Conference on Earthquake Engineering. Vancouver, B.C., Canada. August 1-6, 2004.* 45, 2004.

Nakamura, Y.: *A Method for Dynamic Characteristics Estimation of Subsurface using Microtremor on the Ground Surface*, Quarterly Report of Railway Technical Research Institute (RTRI), 30, 1., 1989.

Neri, G., Caccamo, D., Cocina, O., and Montalto, A.: *Geodynamic implications of earthquake data in the southern Tyrrhenian sea*, Tectonophysics, 258 (1-4), 233-249, 1996.

Neri, G., Barberi, G., Orecchio, B., and Mostaccio, A.: *Seismic strain and seismogenic stress regimes in the crust of the southern Tyrrhenian region*, Earth and Planetary Science Letters, 213 (1-2), 97-112, 2003.

Nigro, F. and Renda, P.: *Forced mode dictated by foreland fault-indenter shape during oblique convergence: the Western Sicily mainland*, Boll. Soc. Geol. It., 121, 151-162, 2002.

Peterson, J.: Observations and modeling of seismic background noise, Open-File Report, 93-322, US Geological Survey, Albuquerque, NM., 1993.

Sambridge, M.: *Geophysical inversion with a neighbourhood algorithm - I. Searching a parameter space*, Geophysical Journal International 103, 4839–4878, 1999.

Schorlemmer, D., Mele, F., and Marzocchi, W.: *A completeness analysis of the National Seismic Network of Italy*, J. Geophys. Res. 115, B04308, doi 10.1029/2008JB006097, 2010.

SESAME Project: *Guidelines for the implementation of the H/V spectral ratio technique on ambient vibrations. Measurements, processing and interpretation*, WP12, deliverable no. D23.12, http://sesame-fp5.obs.ujf-grenoble.fr/Papers/HV_User_Guidelines.pdf, (2004).

Tinti, S. and Mulargia, F.: *Confidence intervals of bvalues for grouped magnitudes*, Bull. Seismol. Soc. Am., 77, 2125-2134, 1987.

Valensise, G. and Pantosti, D.: *A 125 Kyr-long geological record of seismic source repeatability: the Messina Straits (southern Italy) and the 1908 earthquake (Ms 7 1/2)*,. Terra Nova, 4 (4), 472-483, 1992.

Wathelet, M.: *An improved neighborhood algorithm: Parameter conditions and dynamic scaling*, Geophysical Research Letters, 35 (9), art. no. L09301, 2008.

Wathelet M., Jongmans D., and Ohrnberger M.:*Surface-wave inversion using a direct search algorithm and its application to ambient vibration measurements*, Near Surface Geophysics, 211-221, 2004.

Yuncha, Z.A. and Luzon, F.: *On the horizontal-to-vertical spectral ratio in sedimentary basins*. Bulletin of the Seismological Society of America. 90, 4, 1101-1106, 2000.

Peak ID	Longitude	Latitude	Frequ. (Hz)	Ampl.	Cluster	Bedrock depth (m)
1	15.066871	38.125908	0.73	4.49	1	73
2	15.063414	38.126892	1.23	7.64	1	39
3	15.059912	38.127903	0.76	3.80	1	42
4	15.057073	38.129833	0.77	8.12	1	
5	15.055261	38.132241	0.82	5.96	1	61
6	15.055074	38.127563	1.03	6.17	1	60
7	15.056796	38.126292	1.00	5.35	1	48
8	15.059567	38.124235	1.00	5.10	1	48
9	15.062717	38.125018	0.84	6.08	1	
10	15.065124	38.124719	0.77	6.48	1	50
11	15.065406	38.121772	0.83	4.21	1	
12	15.062658	38.12299	0.93	4.68	1	45
13	15.064252	38.119654	1.53	6.00	1	64
14	15.060934	38.121026	1.10	3.56	1	
15	15.057181	38.12165	1.83	3.22	2	
16	15.054749	38.118991	0.90	4.28	3	33
17	15.05174	38.122412	0.90	2.57	3	32
18	15.049392	38.119468	0.87	2.60	3	31
19	15.046962	38.114408	0.87	3.12	3	
20	15.051695	38.116305	0.97	4.00	3	29
21	15.054697	38.11428	0.87	3.31	3	
22	15.050217	38.111984	0.87	4.10	3	
23	15.058505	38.11805	0.77	3.83	1	
24	15.062717	38.125018	1.10	7.09	1	53
25	15.065124	38.124719	1.10	4.30	1	
26	15.059912	38.127903	1.13	4.23	1	
27	15.050217	38.111984	1.23	5.39	2	25
28	15.058505	38.11805	1.30	3.63	1	
29	15.060934	38.121026	1.37	2.55	1	
30	15.054697	38.11428	1.37	4.41	2	
31	15.065406	38.121772	1.43	4.51	1	
32	15.051695	38.116305	1.43	4.54	2	31
33	15.049392	38.119468	1.50	2.67	2	
34	15.054749	38.118991	1.53	4.35	2	43
35	15.05174	38.122412	1.70	3.24	2	
36	15.059567	38.124235	1.78	3.19	2	
37	15.046962	38.114408	2.20	4.23	2	
38	15.060934	38.121026	1.73	2.71	2	39
39	15.054697	38.11428	1.73	4.31	2	
40	15.05174	38.122412	2.67	4.94	2	42
41	15.046962	38.114408	6.08	2.80	4	60
42	15.054749	38.118991	10.14	3.10	4	

Tab. 1 – Peak ID, UTM coordinates, frequencies of the significant peaks, H/V ratios, cluster number and bedrock depth. All reported peaks respect standard deviation criteria for a reliable H/V peak (SESAME, 2004).

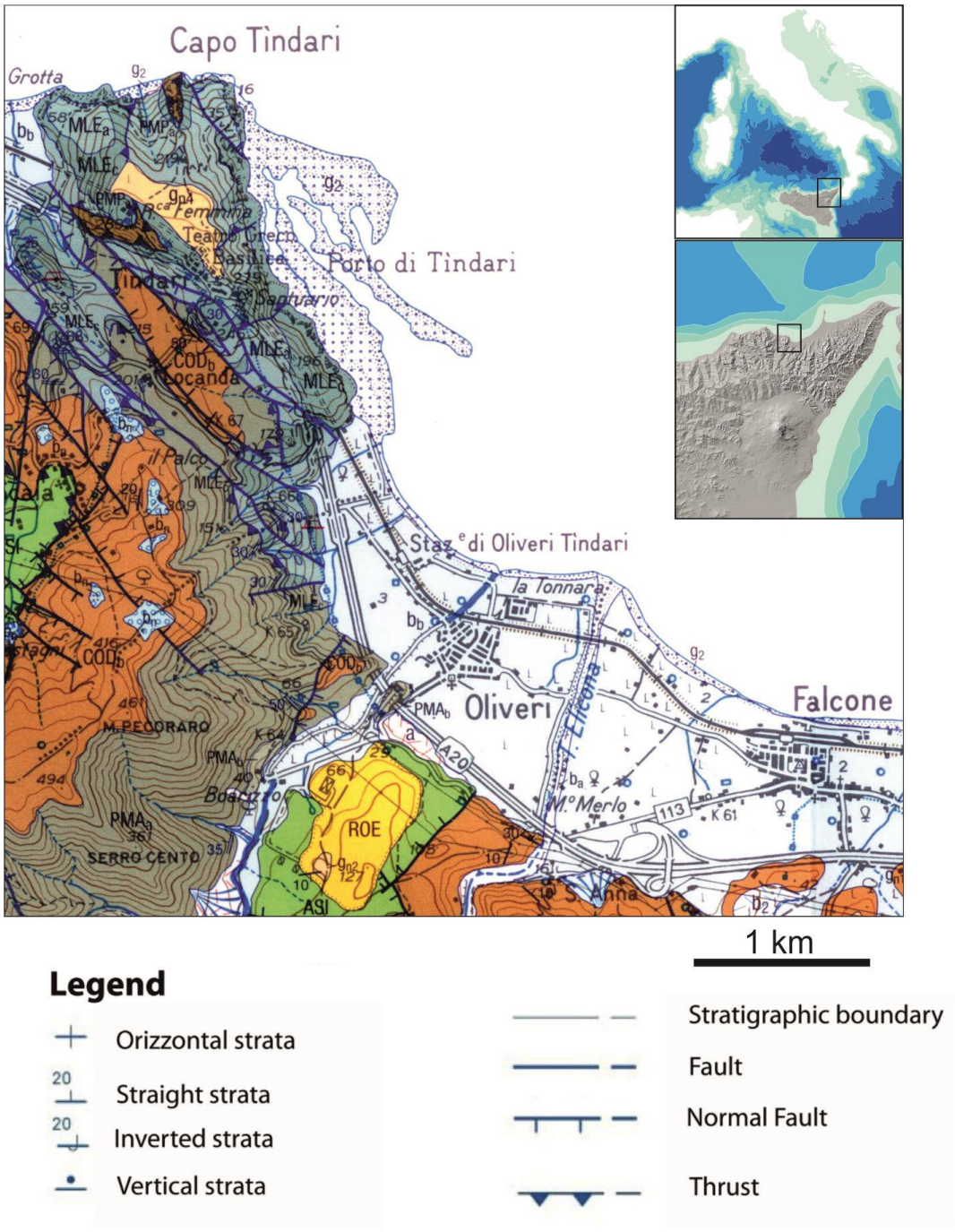

Fig. 1 - Geological map of Oliveri town (from SERVIZIO GEOLOGICO D'ITALIA (2011) - "Foglio Geologico 600 Barcellona Pozzo di Gotto" 1:50.000 CARG-ISPRA): **a**) slope debris; **b_a**) active alluvial deposits; **b_b**) alluvial and litoral deposits; **b_2**) eluvium and colluvium; **b_n**) inactive alluvial terraced deposits; **g_2**) active strandlines (beaches); **g_{n1-5}**) terraced marine deposits; **ROE** Biodetrital calcarenites, clays and sandy clays (Rometta Fm., Upper Pliocene - Middle Pleistocene); **ASI**) Argille Scagliose (Upper Cretaceous); **COD_{b-c}**) Capo d'Orlando Flysch: areanaceous facies (arkose) with alternation of clay-marly levels (Upper Oligocene – lower Burdigalian); **PMA_{a-b}**) paragneiss and gneissic micaschists, silicate marbles, quartzites and aplo-pegmatitic dykes (**PMP_a**) (Apromonte unit – Paleo-Proterozoic – Permian); **MLE_{a-b-c}**) Paragneiss, micaschists, marbles, eclogites, quartzites (Mela unit – Paleozoic).

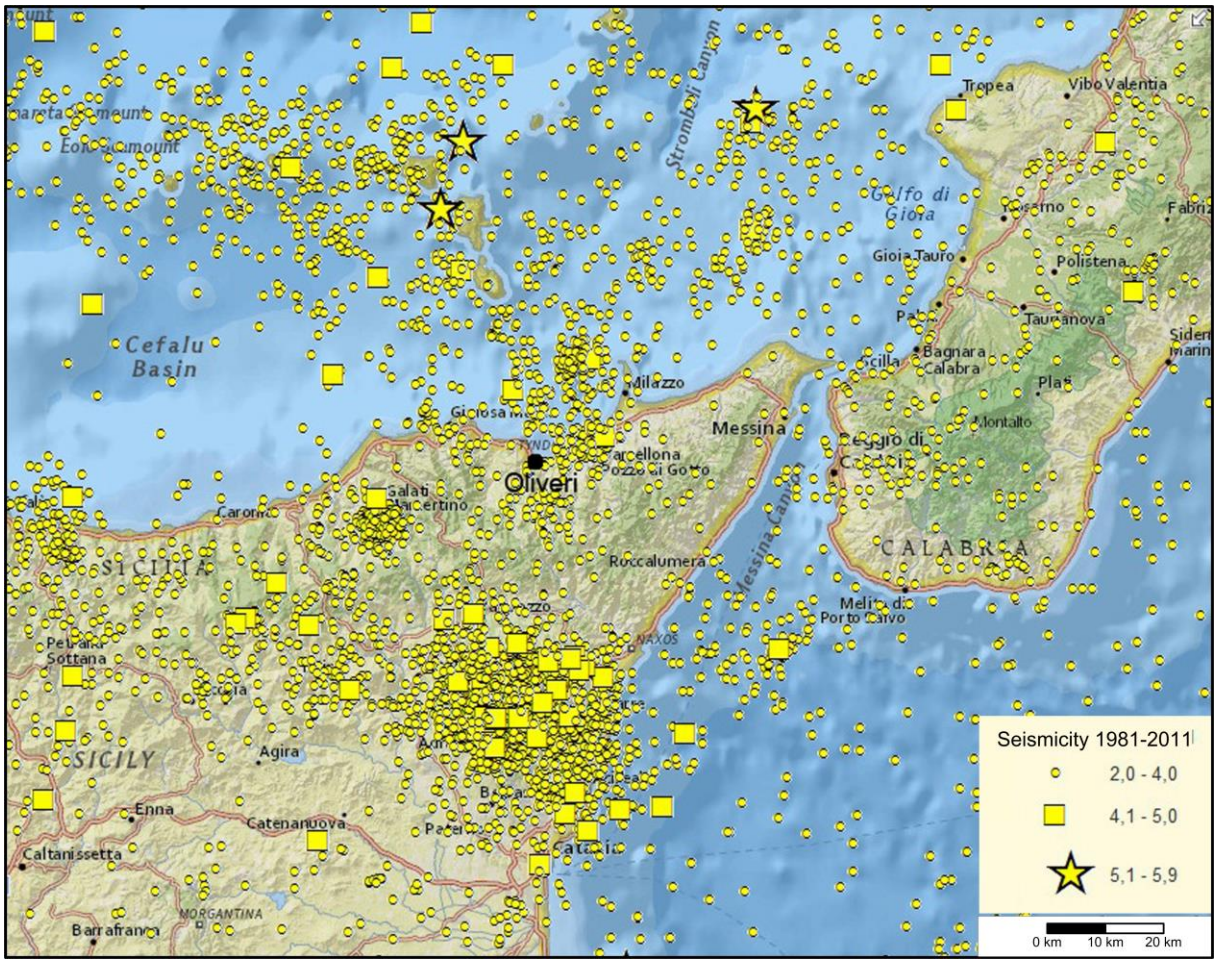

Fig. 2 - Distribution of epicenters of instrumental earthquakes located by the INGV between 1981 and 2011.

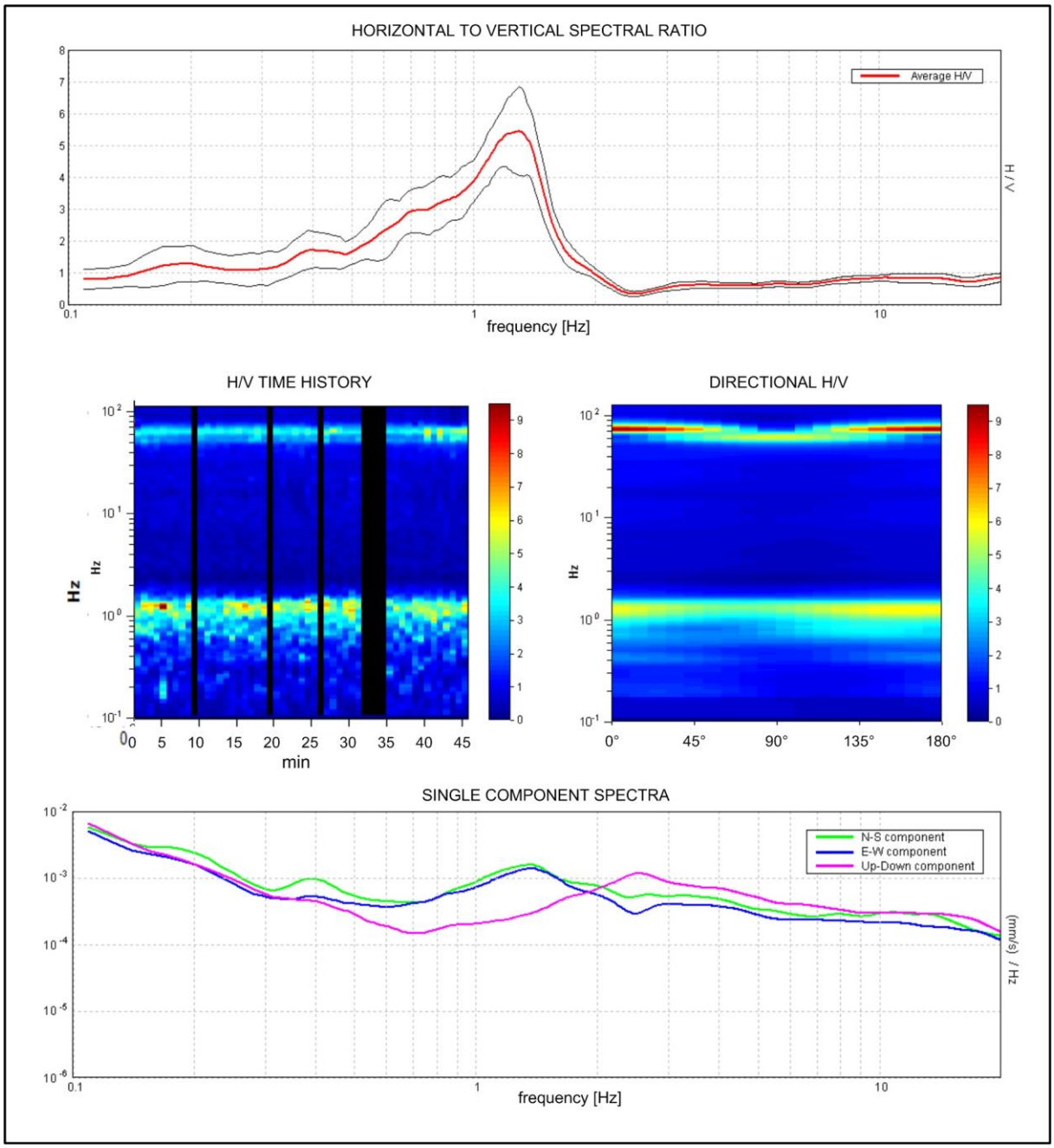

Fig. 3 – HVSR analysis of the microtremor record nr. 7.

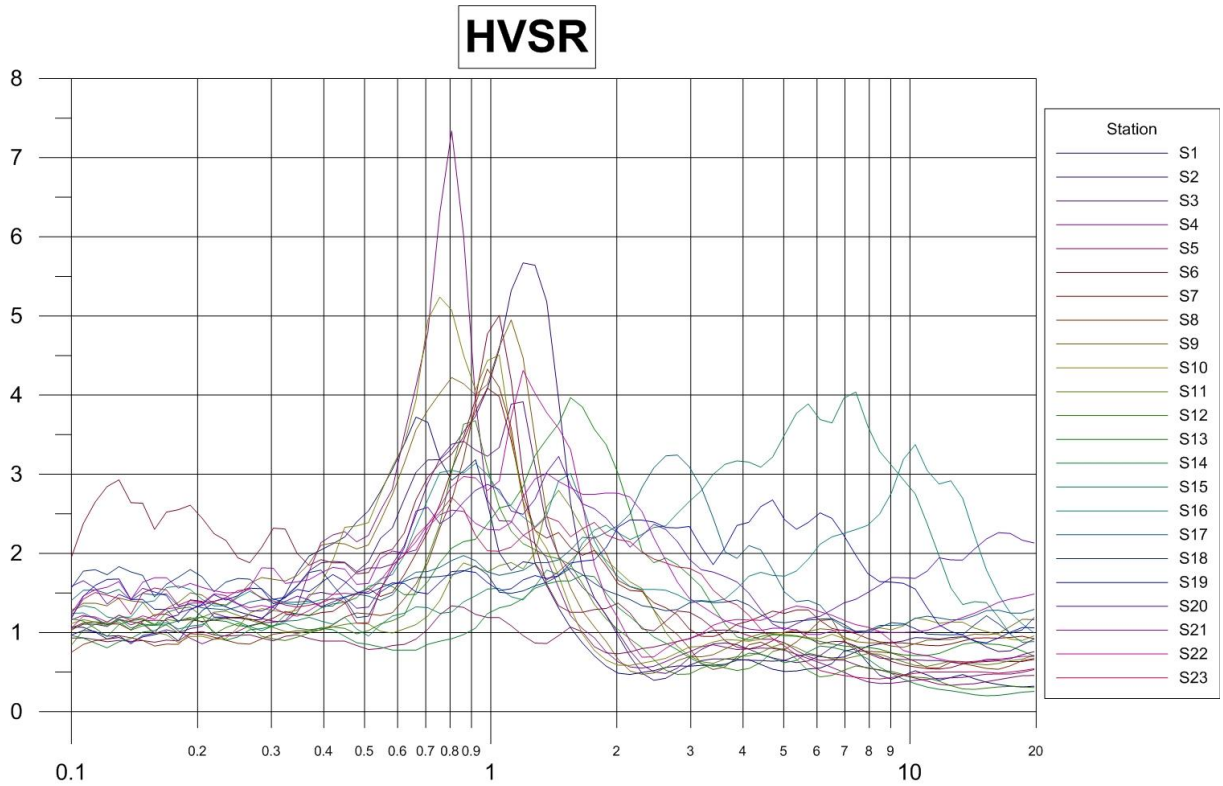

Fig. 4 – HVSR average curves of the clusters in which have been considered to be dominant the structural effects of 23 measures in the area of Oliveri.

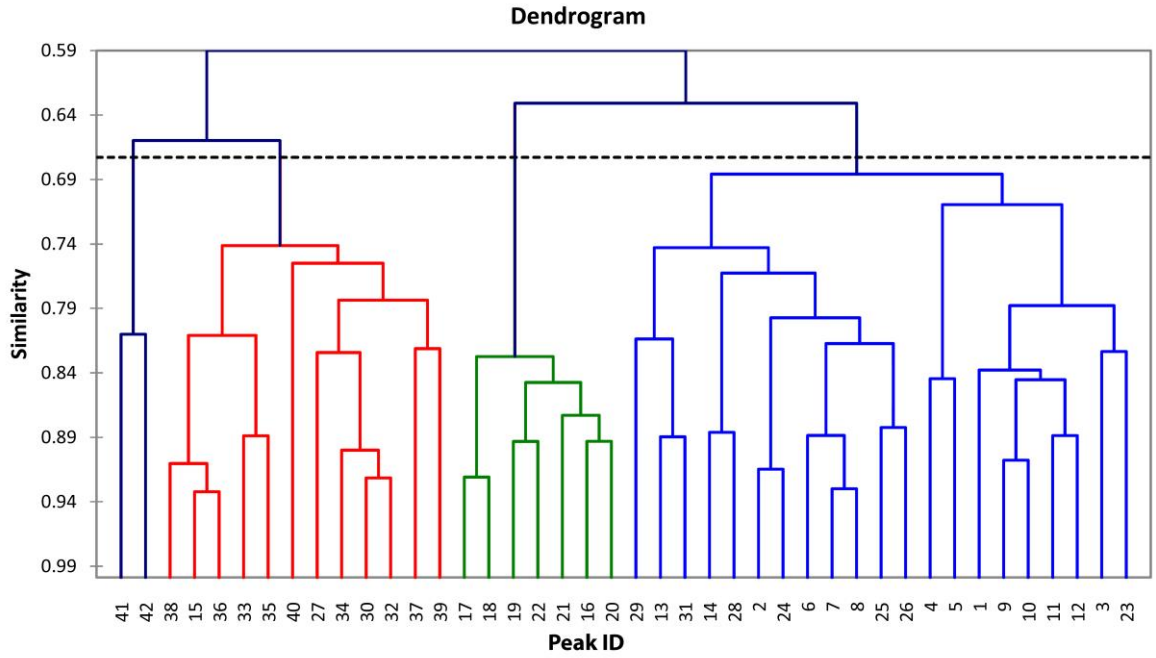

Fig. 5 – Dendrogram of the clustering process.

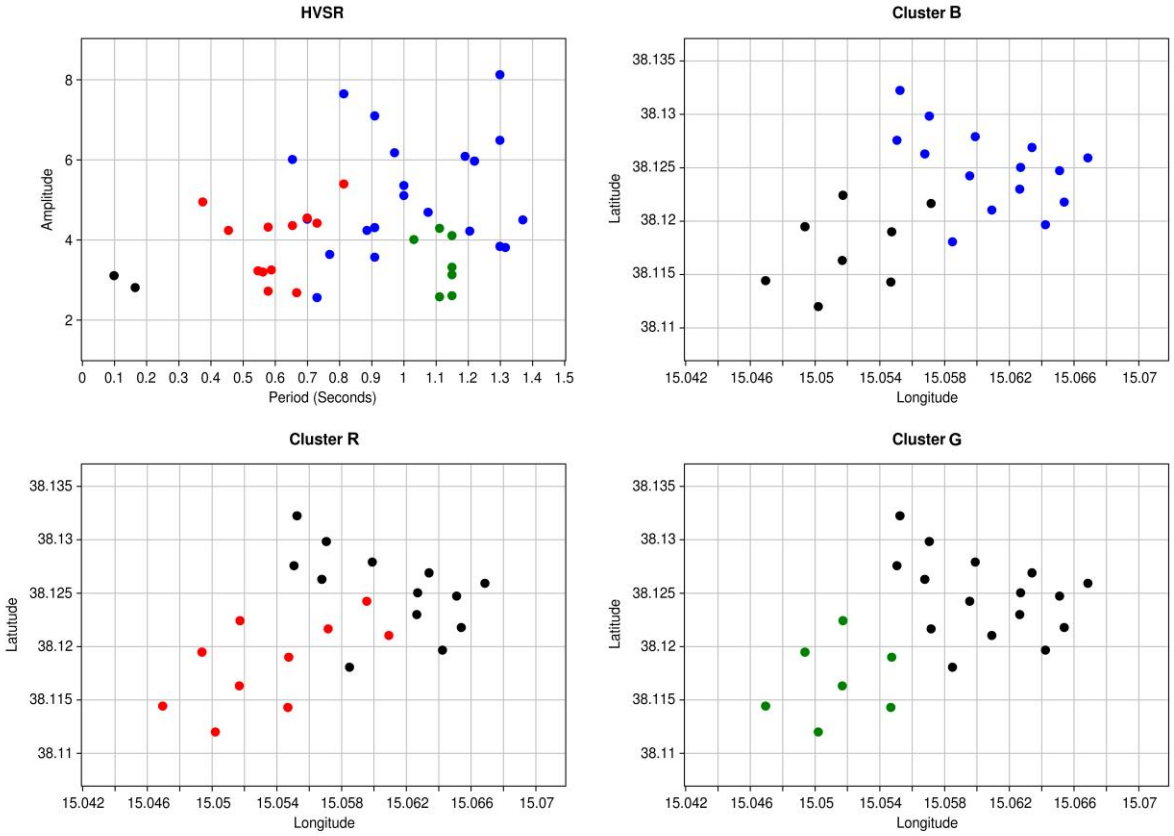

Fig. 6 – Scatter plot of amplitude versus peak period for the four HVSR clusters and spatial distributions of three major ones.

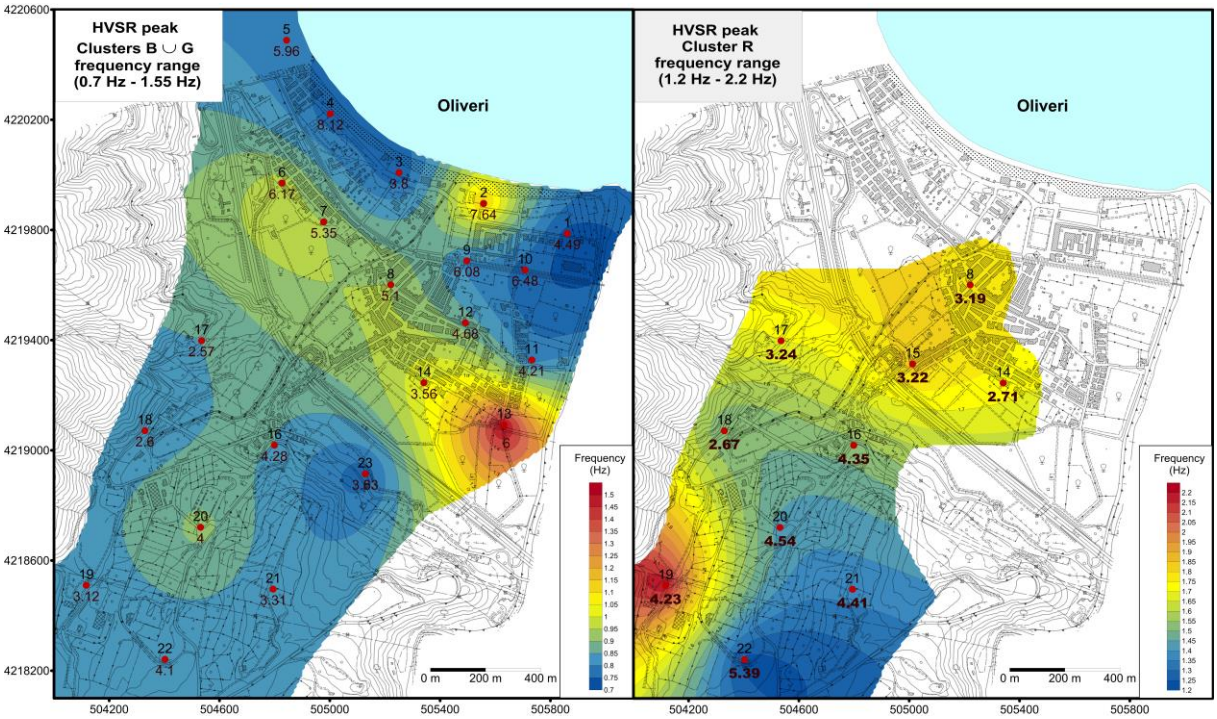

Fig. 7 – HVSR peak frequency maps of cluster B ∪ G (left) and cluster R (right). The coordinate system is WGS84 UTM.

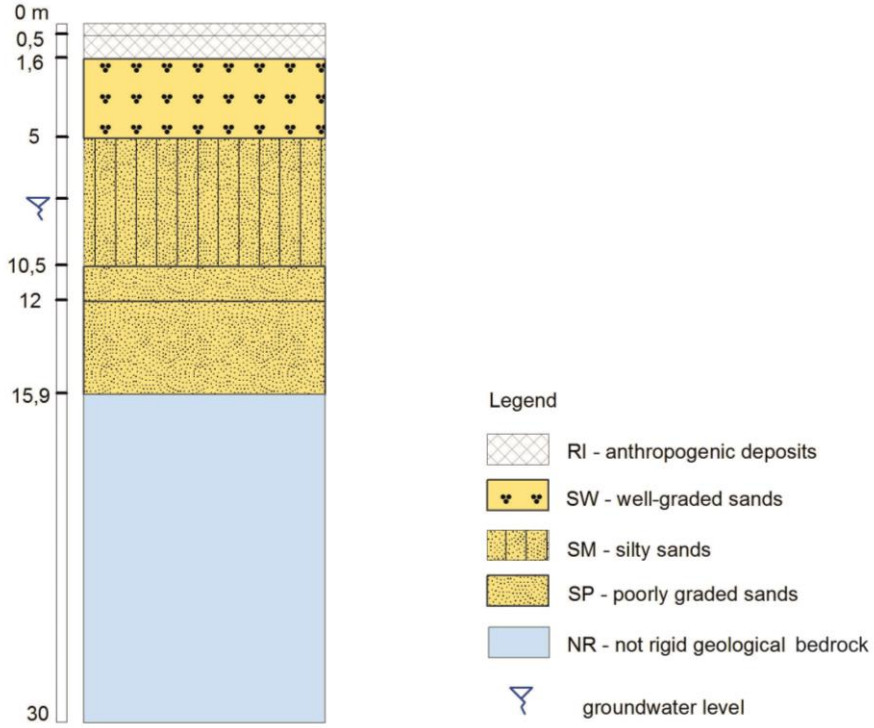

Fig. 8 – Stratigraphic column of the borehole close to Torrente Elicona.

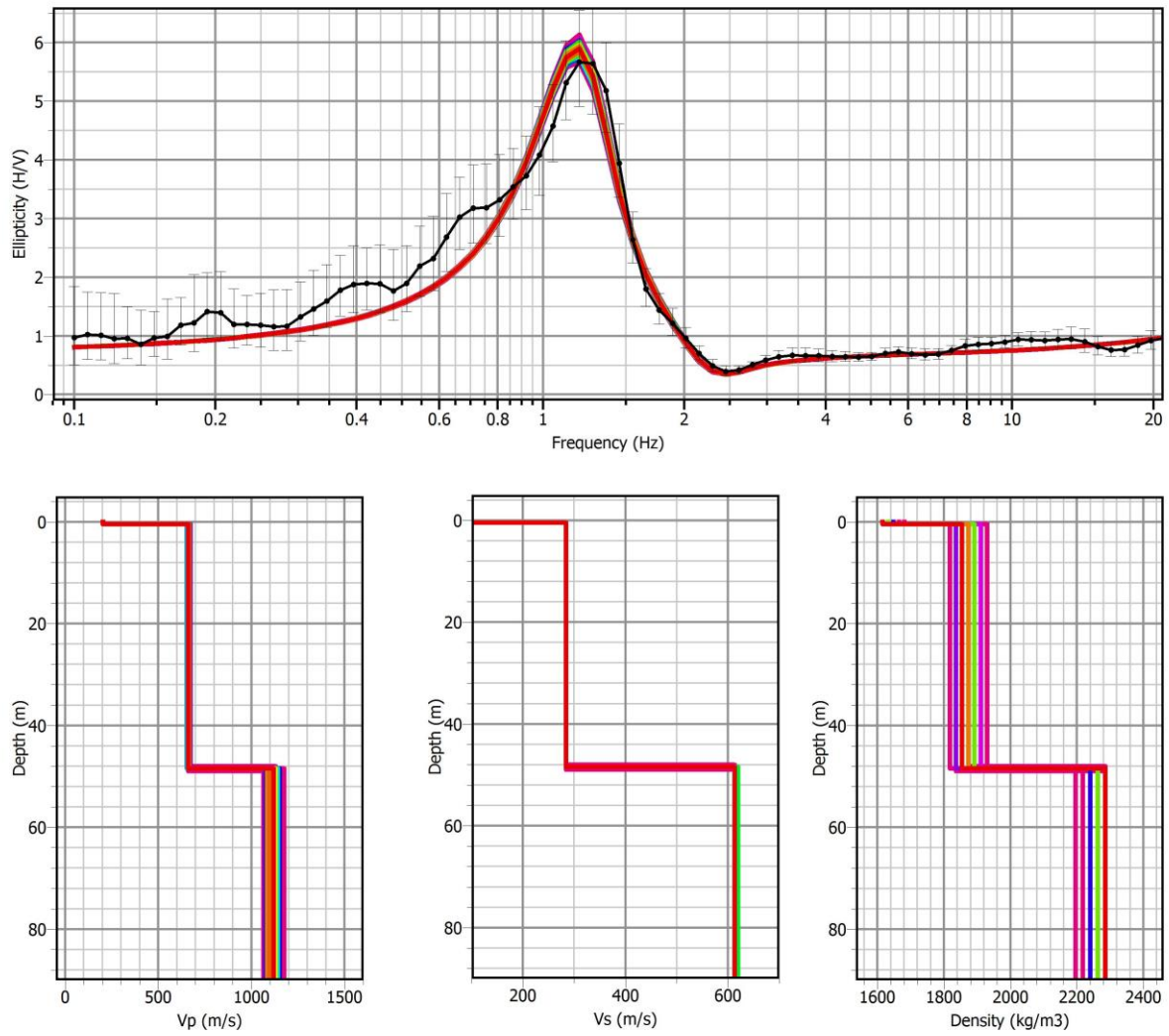

Fig. 9 – Inversion of the HVSR ellipticity curve of the measurement point n.7. Only the models and theoretical H/V curves with misfit values less than 1.09 are plotted.

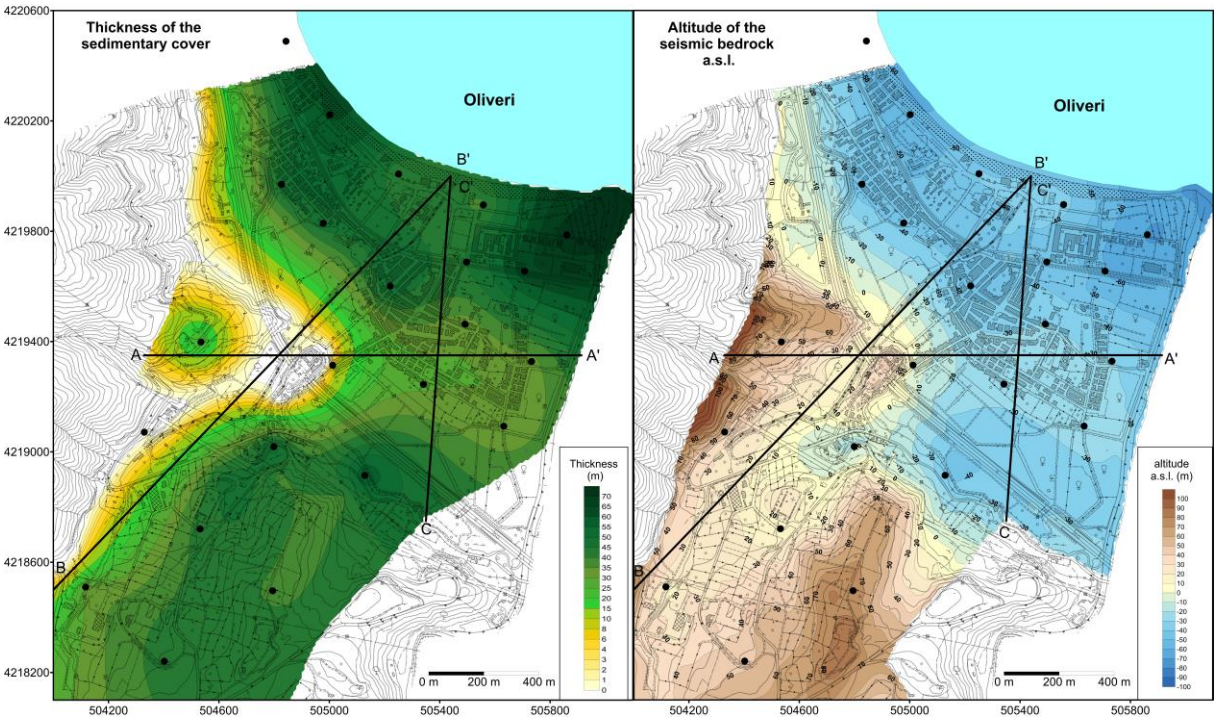

Fig. 10 – Oliveri. Left) Map of the thickness of the sedimentary cover. Right) Map of the altitude of the seismic bedrock above sea level. The coordinate system is WGS84 UTM.

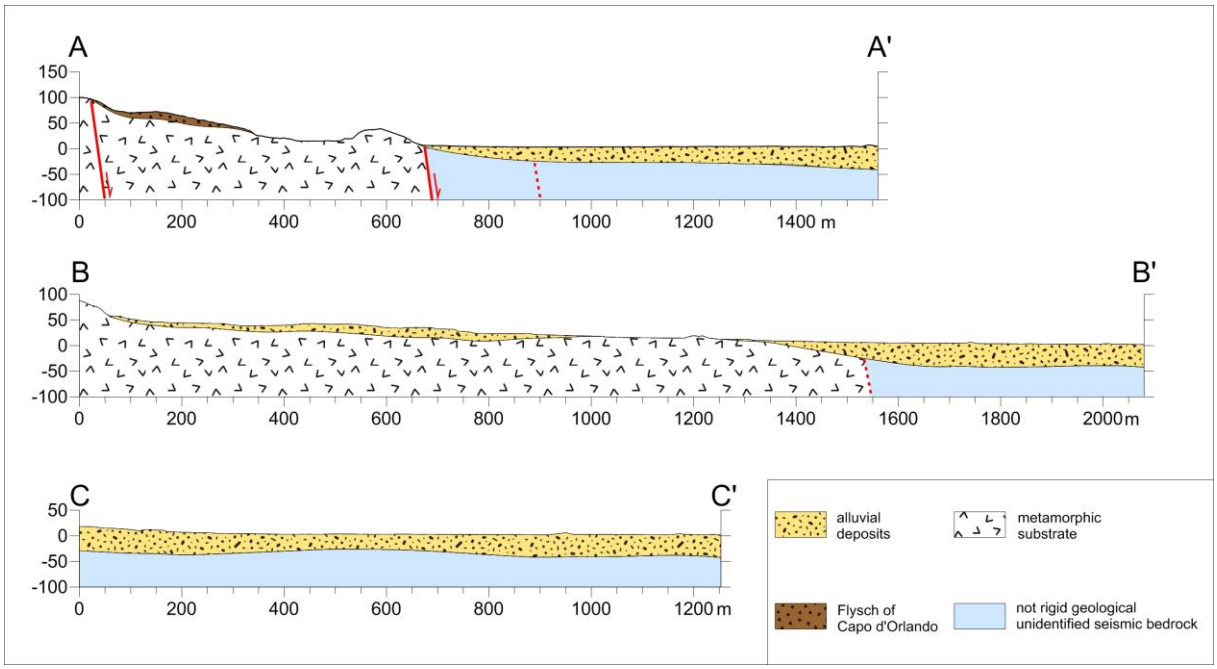

Fig. 11 – Oliveri. Sections representing the seismic bedrock and the soft cover. The tracks of the sections are plotted in fig 10.